https://doi.org/10.17221/59/2019-SWR

Adsorption of selected azo dyes from an aqueous solution by activated carbon derived from *Monotheca buxifolia* waste seeds

Ruqia Nazir, Muslim Khan[1], Riaz Ur Rehman[1], Shaukat Shujah[1], Mansoor Khan[1], Mohib Ullah[1,2], Amir Zada[2,3]*, Nasir Mahmood[4], Irshad Ahmad[5]*

[1]*Department of Chemistry, Kohat University of Science and Technology, Kohat, Pakistan*
[2]*Key Laboratory of Functional Inorganic Material Chemistry, Ministry of Education, School of Chemistry and Material Science, Heilongjiang University, Harbin, P.R. China*
[3]*Department of Chemistry, Abdul Wali Khan University Mardan, Mardan, Pakistan*
[4]*Key Laboratory of Saline-alkali Vegetation Ecology Restoration, College of Life Sciences, Northeast Forestry University, Harbin, P.R. China*
[5]*Institute of Basic Medical Sciences, Khyber Medical University Peshawar, Peshawar, Pakistan*

**Corresponding authors: ruqianazir@yahoo.com; amistryoo9@yahoo.com*

Citation: Nazir R., Khan M., Ur Rehman R., Shujah S., Khan M., Ullah M., Zada A., Mahmood N., Ahmad I. (2020): Adsorption of selected azo dyes from an aqueous solution by activated carbon derived from *Monotheca buxifolia* waste seeds. Soil & Water Res., 15: 166–172.

Abstract: In this study, activated carbon derived from *Monotheca buxifolia* waste seeds was used for the adsorptive removal of a number of selected azo dyes such as Eriochrome Black T (EBT), Remazol brilliant blue (RBB), Remazol yellow (RY) and Remazol brilliant orange (RBO) from an aqueous solution by changing the initial dye concentration, adsorbent dosage, solution pH, contact time and temperature. A Fourier transform infrared spectroscopic analysis of the activated carbon showed the existence of hydroxyls, methyl, methylene, carbonyls, alkane and alkenes groups while the scanning electron microscopic image displayed the gradual formation of cavities and open pores on the surface. The results showed that as the amount of the adsorbent and the shaking time were increased, the removal percentage of the dye increased accordingly. Higher adsorption percentages were observed at a lower dye concentration and temperature in an acidic media at a pH range (1–5). The investigated data were evaluated with the Langmuir and Freundlich adsorption models. The maximum adsorption capacities obtained from the Langmuir model were 112.36, 96.34, 97.65 and 90.91 mg/g for EBT, RBB, RY and RBO, respectively. The results indicated that the electrostatic interaction was the main cause of the adsorption of these anionic azo dyes on the surface of the activated carbon.

Keywords: active sites; Freundlich isotherm; Langmuir isotherm; pH

The release of dyes into wastewater from dying industries poses severe environmental risks and has adverse effects on aquatic and terrestrial life. Synthetic dyes, particularly azo dyes, with one or more azo bonds (-N=N-) are the back bones of the textile industry. These dyes possess complex molecular structures and are non-biodegradable. Some of them are carcinogenic and mutagenic and chronic exposure to their high concentrations can result in considerable damage to the immune, nervous and reproductive systems (Ali et al. 2018a, 2019; Xu et al. 2019). Keeping their hazardous effects in view, it is very important to remove them before they are discharged to the external environment.

Different techniques and methods such as photocatalysis, advanced oxidation, electrochemical

https://doi.org/10.17221/59/2019-SWR

treatment, precipitation, solvent extraction, reverse osmosis and coagulation/flocculation have been used to remove coloured contaminates from industrial effluents (Ali et al. 2018b; Zada et al. 2018; Hisada et al. 2019; Kang et al. 2019). However, these methods have low efficiencies, high operational energy and produce secondary pollutants (Ullah et al. 2020). It is therefore of much importance to develop cheap, cost effective and efficient methods to treat these dyes for environmental remediation. Among all the treatment techniques, adsorption is a simple and low-cost effective technique. For this purpose, extensive varieties of adsorbents are available to remove the dyes from wastewater. Amongst them, activated carbon can be even more effective because of its porous nature and high surface area and it can be used for the removal of both liquid and gas pollutants (Zhou et al. 2019). Low cost, renewable and highly activated carbon from agricultural waste is receiving worldwide attention these days. Different agricultural wastes such as corncobs, banana/orange peels, bamboo dust, bagasse, cassava peels, palm shells, hazelnuts, coconut shells, etc. have been applied as activated carbon precursors (Nosheen et al. 2000). The seed of *Monotheca buxifolia*, locally called Gurguri, is a new source of agricultural waste domestically used as a combustion material or randomly disposed of. Keeping its disposal problems and large-scale availability in view, an effective adsorbent was developed through the carbonisation from the waste seeds of the *Monotheca buxifolia* plant and was applied for the removal of selected azo dyes from aqueous solutions along with the investigation of the effects of its various physical parameters. The data obtained were applied to the Langmuir and Freundlich adsorption isothermal models. We hope that this study will not only reduce the disposal problem of the *Monotheca buxifolia* waste seeds, but it will also provide a low-cost activated carbon adsorbent for the removal of dyes from wastewater for environmental remediation.

MATERIAL AND METHODS

Preparation of the adsorbent. The *Monotheca buxifolia* fruits were obtained from a local fruit market of the Karak district, Pakistan and their seeds were washed thoroughly with distilled water and ethanol. The well cleaned seeds were dried in oven at 100 °C for 24 h and then ground with the help of a pestle and mortar into a fine powder. The powdered seeds were first impregnated with a 20% $ZnCl_2$ solution and then washed with distilled water and dried. The obtained materials were carbonised in a furnace at 530 °C for half an hour to get the activated carbon (Ullah et al. 2020). The obtained adsorbent was pulverised and sieved to a size of 100 µm for the removal of the azo dyes. The effect of the various factors such as the initial dye concentration, adsorbent dosage, temperature, pH and contact time were examined for the adsorptive removal of the different azo dyes with the as-prepared activated carbon obtained from *Monotheca buxifolia*.

Preparation of the dye solutions. Stock solutions of the selected dyes including Eriochrome Black T (EBT), Remazol brilliant blue (RBB), Remazol yellow (RY) and Remazol brilliant orange (RBO) with an initial concentration of 1 000 ppm were prepared by dissolving them in distilled water. The as-prepared solutions were used for the preparation of other solution by the dilution method and stored for further experimental work.

Characterisation techniques. A SEM micrograph of the activated carbon was obtained with a scanning electron microscope (SEM, Model JSM 5910, JEOL, Japan). The Infrared spectra of the powdered seeds and activated carbon samples were determined with the Fourier Transform Infrared Spectroscopy (FTIR, TM Spectrum 2000, Japan) in the range of 4 000–400 cm^{-1} using the potassium bromide (KBr) pellet method. The point to zero charge (PZC) was determined on the surface of the activated carbon samples by using the distilled water method. 40 ml of the distilled water was taken in 11 different reaction flasks and the initial pH was adjusted between a pH of 2 and 12 with a 0.1 M NaOH/HCl solution. 0.1 g of activated carbon was added to each flask and placed in a shaker for 24 h at 120 rpm at 298 K. After agitation, the solutions were filtered and the final pH was measured. The difference in the pH was calculated from the difference of the final and initial pH values and the PZC was determined.

Adsorption experiments. 50 ml aqueous solutions of the different concentrations of each dye were agitated with a given amount of adsorbent using a Bath Wise Shaker (WSB-30, Daihan Scientific, Korea) at 120 rpm. The different experimental parameters such as initial dye concentration (10–100 ppm), adsorbent dose (0.1–0.6 g/50 ml), pH (1–13), temperature (293–323 K) and time of contact were checked to evaluate the optimum conditions for the maximum adsorption of the azo dyes from the 50 ml aqueous solution under the given conditions. After agitation,

https://doi.org/10.17221/59/2019-SWR

each solution was filtered with Whatman paper No. 42 and the absorbance of the dye was measured. The removal percent of the dyes was determined with the help of the following equation.

$$\% \text{ removal} = C_o - C_e/C_o \times 100 \quad (1)$$

where:

C_o, C_e – the initial and equilibrium concentrations of the dye.

RESULTS AND DISCUSSION

Characterisation of the adsorbent

The SEM images were taken to observe the morphology of the activated carbon. Figure 1A illustrates the micrograph of the activated carbon (at the optimised conditions) of 10 000× magnification. The surface morphology of the activated carbon shows cavities and open pores on its surface.

The FTIR spectra were applied to characterise the functional groups present on the surface of the *Monotheca buxifolia* seed and its derived activated carbon and the results are shown in Figure 1B. It is clear that most of the spectra of the *Monotheca buxifolia* seed is linear showing the presence of a lignin backbone. Two small peaks at 2 918 and 2 848 cm^{-1} suggest symmetric and asymmetric stretching vibrations of the C-H groups. A peak at 1 588 cm^{-1} is attributed to the conjugated C=C in the aliphatic and aromatic bonds (Tariq et al. 1996). The spectra of the activated carbon shows a band at 3 308 cm^{-1} which can be assigned to the stretching vibration of O-H, the presence of peaks at 3 000–2 853 cm^{-1} indicate the symmetric and asymmetric C-H stretching in methylene and methyl while the sharp absorption peak at 1 743 cm^{-1} suggests the stretching vibrations of the C=O functional group. The band at 1 645 cm^{-1} may be due to the bending vibrations of the OH group. The band at 1 457 cm^{-1} shows the asymmetric and symmetric bending of C-H, the peak at 1 376–1 316 cm^{-1} indicates the bending of the CH_3 group while the presence of the peak at 1 028 cm^{-1} represents the stretching vibration of cellulose/hemicellulose and the ary-OH group in the lignin (Iqbal et al. 2015).

The point to zero charge (PZC) was tested to find out the charges on the surface of the adsorbent. The charge on the surface of the activated carbon depends on the interactions of the H^+ and OH^- present in the solution. The activated carbon may possess either a positive or negative charge depending on the concentration of the H^+ and OH^- ions present on its surface. The value of pH_{ZPC} is 5.95 for the activated carbon derived from the seeds of *Monotheca buxifolia*, as shown in Figure 2A. It is clear that the initial pH values are slightly higher than that of the final pH values. It makes the adsorbent surface slightly positively charged. Under these conditions, the hydroxyl group (OH^-) increases in number and starts to form a counter-ion layer that is close to the surface. As a result, the proton (H^+) will make a double layer via diffusion which subsequently decreases the pH values.

Optimisation of the adsorption parameters

Effect of the initial dye concentration. In order to determine the effect of the dye concentration on their removal, 0.2 g of the adsorbent was shaken with

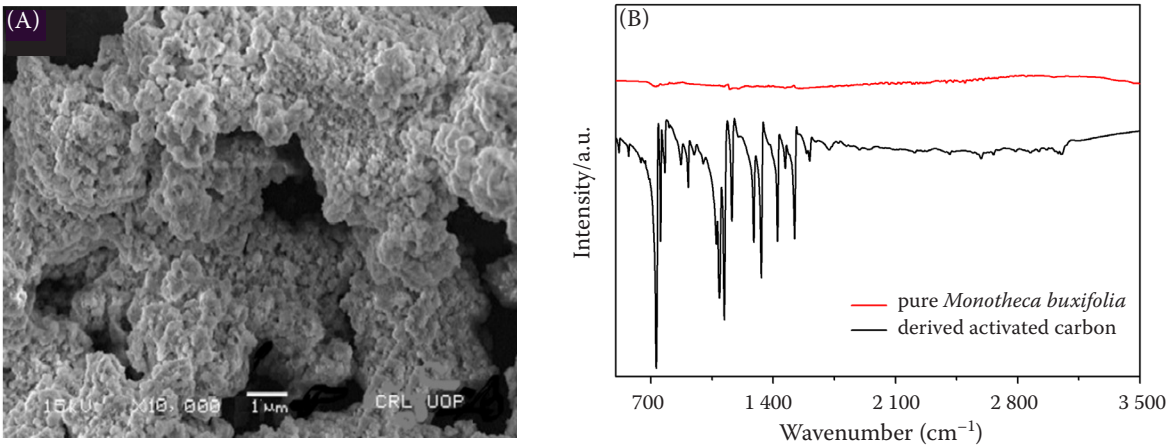

Figure 1. The scanning electron microscopy (SEM) image of the as-prepared adsorbent (A) and the Fourier transform infrared (FTIR) spectra of the pure *Monotheca buxifolia* seeds and the derived activated carbon (B)

https://doi.org/10.17221/59/2019-SWR

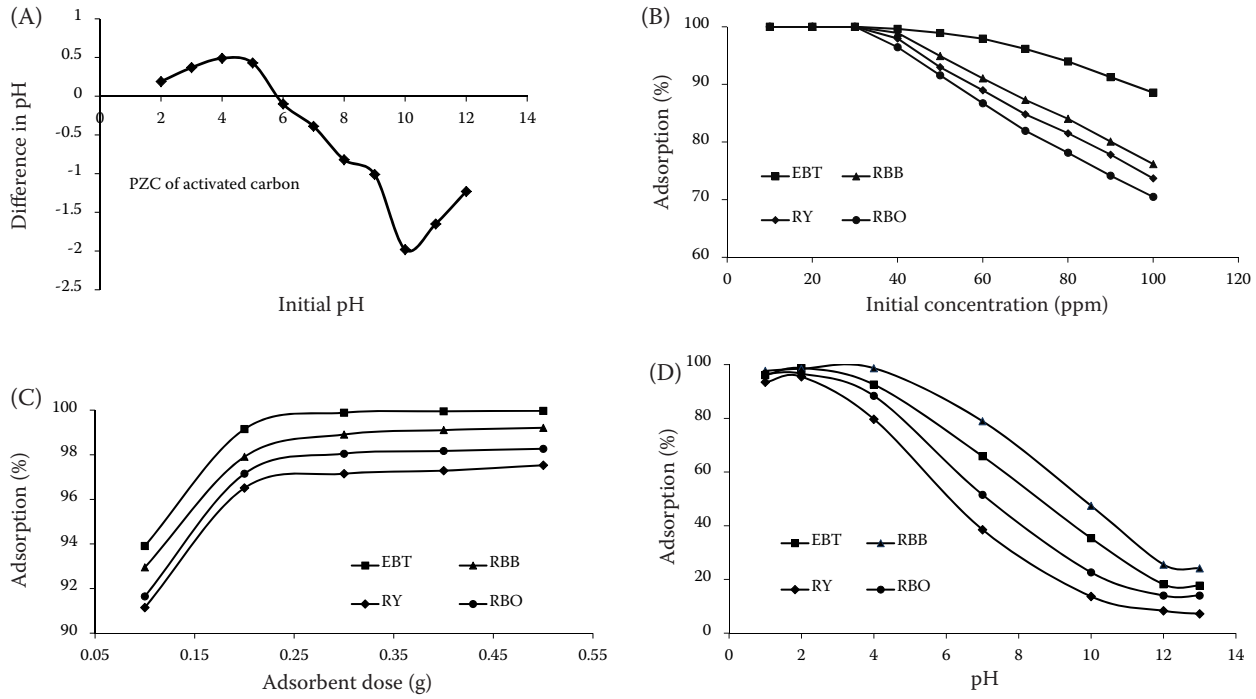

Figure 2. The point zero charge (PZC) of the adsorbent (A), the effect of the initial dye concentration (B), the adsorbent dose (C) and the pH on the adsorption of the selected dyes over the activated carbon (D)
EBT – Eriochrome Black T; RBB – Remazol brilliant blue; RY – Remazol yellow; RBO – Remazol brilliant orange

different initial concentrations of the dyes and the results are shown in Figure 2B. It is clear that for all the dyes, their removal efficiencies decrease when their concentrations increase. This is because, at lower concentration, the number of dye particles is low when compared to the available active sites on the surface of the adsorbent, therefore, the adsorption is more frequent. When the concentration is increased, more dye molecules are crowded onto the surface of the adsorbent and the active sites are quickly occupied by them. Thus, equilibrium between the adsorbed and non-adsorbed dye particles is established which reduces the removal efficiency. Clearly, the decline trend in the adsorption is different for the different dyes. It is somewhat lower for Eriochrome black T and higher in the case of Remazol brilliant blue dye. This effect is attributed to the different structures of the azo dyes as these have different interactions with the same adsorbent.

Effect of the adsorbent concentration. The adsorption efficiency strongly depends on the dosage of the adsorbent and increases as the amount of the adsorbent increases. In the present study, we increased the amount of the adsorbent from 0.1 g to 0.2 g and the effect on the adsorption was measured under the identical initial dye concentration. It is clear from Figure 2C that as the adsorbent dosage increases, the removal percent of all the dyes under investigation also increases. This increase in the adsorption is attributed to the large number of the available adsorption sites, as the amount of adsorbent increases. Thus, more dye molecules are adsorbed and are effectively removed which improves the adsorption efficiency. This result also supports our above statement about the interaction of the different structural dyes with our adsorbent, as the maximum adsorption is achieved in the case of the EBT dye as compared to the RBB dye with minimum adsorption.

Effect of the pH. The pH of solution has closed relationship with the interaction of the adsorbent and the adsorbate particles as it strongly determines the magnitude of the charge on the surface of the adsorbent. In this study, we changed the pH of the solution from 1–13 by adding 0.1 M NaOH/HCl under the identical initial dye concentration and the adsorbent dosage and the % removal efficiency was studied as shown in Figure 2D. It is clear that for all the dyes, the removal efficiency is high between a pH of 1–3 and constantly decreases as the pH increases from 5–13. Interestingly, the effect of the pH is different for the different dyes. The re-

https://doi.org/10.17221/59/2019-SWR

moval efficiency of EBT is maximum at pH 2 while RBB, RY and RBO show maximum adsorption at the pH values of 3, 2 and 1, respectively. It is obvious that at a lower pH, the surface of the adsorbent is positively charged and its electrostatic interaction with the negatively charged dye anions is strong, resulting in the high removal of the dye particles. As the pH is increases, the surface of the adsorbent gradually acquires a negative charge. As a result, the electrostatic repulsion between the adsorbent and the adsorbate particles is established which badly decreases the overall removal efficiency.

Effect of the contact time. Figure 3A reveals that the rate of adsorption increases gradually with an increase in the shaking time and the optimum removal efficiency for all the selected dyes is achieved in 3 h. A further increase in the shaking time does not show any substantial change in the equilibrium concentration. This is simply explained on the basis of the available adsorption sites for the dye molecules. Initially, a large number of surface sites are available for the adsorption. As time increase, more and more surface sites are occupied and the number of available sites decreases which prevents the occupation of more dye particles. At the equilibrium after 3 h, the number of adsorption sites are completely occupied and there is no more available space to adsorb more molecules. Thus, the adsorption gains its optimum value.

Effect of the temperature. The variation in the temperature strongly affects the removal efficiency of the dye particles by adsorption. For effective adsorption, the interaction between the adsorbent and the adsorbate particles must be appreciable. Since, at low temperature, the kinetic energy is low and the intermolecular attractive forces are strong, therefore, the adsorbate molecules are easily and strongly attracted to the surface of the adsorbent resulting in more pronounced adsorption. When temperature increases, the kinetic energy increases and the intermolecular interaction between the adsorbate and the adsorbent particles decreases. Thus, the adsorbate molecules are gradually desorbed from the surface of the adsorbent to decrease the rate of

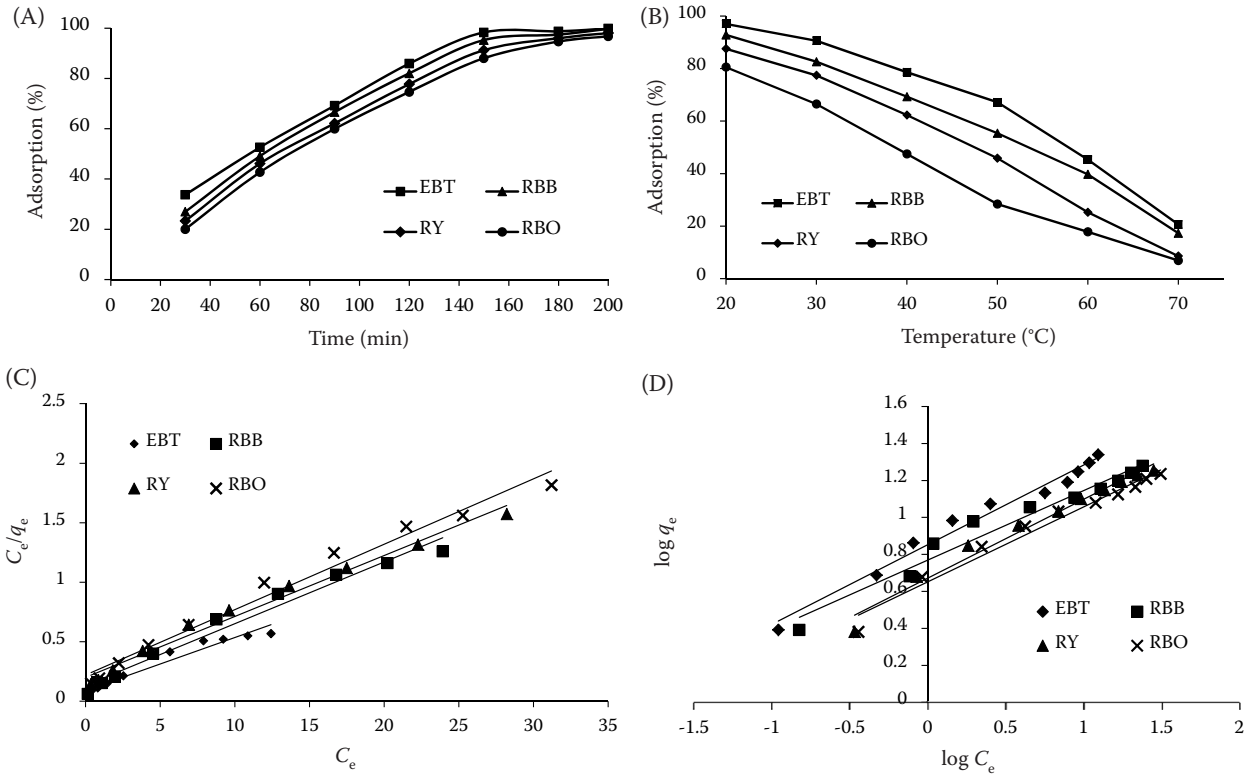

Figure 3. The effect of the contact time (A) and the temperature (B) on the adsorption of the selected dyes over the activated carbon, the Langmuir isotherms (C) and the Freundlich isotherms for the adsorption of the selected dyes over the activated carbon (D)

EBT – Eriochrome Black T; RBB – Remazol brilliant blue; RY – Remazol yellow; RBO – Remazol brilliant orange

https://doi.org/10.17221/59/2019-SWR

Table 1. The Langmuir and Freundlich coefficients for the adsorption of the dyes on the adsorbate

Adsorbate	Langmuir coefficients			Freundlich coefficients			
	Q_m (mg/g)	K_L (mg/l)	R^2	K_f (mg/g)	$1/n$	N	R^2
EBT	112.36	0.318 3	0.950 5	2.345	0.430 6	2.32	0.979 7
RBrB	96.34	0.394 3	0.969 5	2.158	0.375 4	2.66	0.972 9
RY	97.65	0.255 4	0.973 9	1.957	0.426 1	2.34	0.975 7
RBrO	90.91	0.249 5	0.959 8	1.918	0.405 4	2.47	0.972 6

EBT – Eriochrome Black T; RBB – Remazol brilliant blue; RY – Remazol yellow; RBO – Remazol brilliant orange

adsorption. As can be seen from Figure 3b, the rate of adsorption decreases as the temperature increases in the case of all dyes. Clearly, the rate of adsorption is high at 303 K. It is obvious that the extent of the adsorbed dye reduces with the rise in temperature. By comparing our results with other similar works, our adsorbent shows an enhanced adsorption activity under the optimal conditions (Abbas 2013).

Adsorption isotherms

In this study, the adsorption equilibrium data were fitted by two isotherm equations including the Langmuir and Freundlich isotherms. The adsorption isotherms for all the dyes under consideration are shown in Figure 3C and 3D as a function of their concentrations at room temperature. The obtained results were checked with the Langmuir and Freundlich equations. The linear form of the Langmuir equation is given by

$$C_e/q_e = 1/q_m K_L + C_e/q_m \quad (2)$$

where:
C_e – dye concentration;
q_e – amount of adsorbate;
q_m – highest monolayer capability;
K_L – constant.

The Freundlich equation is given by

$$\log q_e = \log K_f + 1/n \log C_e \quad (3)$$

where:
q_{eq} – amount of adsorbate;
K_f – constant equal to the intercept of the plot.

The value of n is obtained from the slope of the plot and shows the intensity of the adsorption. From the plots of log q_e versus log C_e, it is clear that the slope $1/n$ ranges between 0 and 1 indicating favourable adsorption of all azo dyes on our adsorbent. It is clear that the values of q_e or log q_e linearly increase with C_e or log C_e indicating the usefulness of both models. The values of K_L and q_m in the Langmuir equation and K_f and n in the Freundlich equation were calculated from the slopes and intercept of the linear graphs and are shown in Table 1. The Freundlich isotherm having a higher value of R^2 ($R^2 > 0.97$) makes it the better fit than the Langmuir isotherm ($R^2 > 0.95$) for all the dyes. The higher values of K_f (1.92 to 2.35 mg/g) and n (2.32 to 2.66) show that the activated carbon has a higher adsorption capacity and affinity for the azo dye molecules and reveals the favourability of the adsorption. The Freundlich model assumes a multilayer adsorption on the surface of the adsorbent. The Langmuir isotherm constants q_m and K_L are 112.36, 96.34, 97.65 and 90.91 mg/g for EBT, RBB, RY and RBO at 30 °C, respectively. The activated carbon had a higher adsorption capacity of 90.91–112.36 mg/g suggesting that it is a promising adsorbent to remove azo dyes from the aqueous solutions.

CONCLUSION

The adsorbent obtained from the waste seeds of *Monotheca buxifolia* (Gurguri) was successfully employed for the removal of the selected azo dyes from an aqueous solution by adsorption. The removal percent of the selected azo dyes were observed to increase with an increase in the shaking time and adsorbent dosage while they were observed to decrease with a decrease in the pH and the initial dye concentration. The concentrations of all the dyes varied from 30 to 100 mg/l with a 0.2 g mass of activated carbon. The maximum adsorption capacities were 112.36, 96.34, 97.65 and 90.91 mg/g for Eriochrome Black T, Remazol brilliant blue, Remazol yellow and Remazol brilliant orange at 30 °C, respectively, and a pH between 1 and 4. The Freundlich isotherm was the best fit for the equilibrium data up to $R^2 = 0.97$ which signifies that a heterogeneous adsorption takes place between the selected azo dyes and *Monotheca*

https://doi.org/10.17221/59/2019-SWR

buxifolia based on the activated carbon and the Freundlich coefficients were higher than $R^2 > 0.96$.

REFERENCES

Abbas F.S. (2013): Dyes removal from wastewater using agricultural waste. Advances in Environmental Biology, 7: 1019–1026.

Ali N., Awais, Kamal T., Ul-Islam M., Khan A., Shah S.J., Zada A. (2018a): Chitosan-coated cotton cloth supported copper nanoparticles for toxic dye reduction. International Journal of Biological Macromolecules, 111: 832–838.

Ali N., Zada A., Muhammad Z., Ismail A., Rafiq M., Riaz A., Khan A. (2019): Enhanced photodegradation of methylene blue with alkaline and transition-metal ferrite nanophotocatalysts under direct sun light irradiation. Journal of the Chinese Chemical Society, 66: 402–408.

Ali W., Ullah H., Zada A., Muhammad K.A., Muhammad W., Muhammad J.A., Nadhman A. (2018b): Effect of calcination temperature on the photoactivities of ZnO/SnO_2 nanocomposites for the degradation of methyl orange. Materials Chemistry and Physics, 213: 259–266.

Hisada M., Tomizawa Y., Kawase Y. (2019): Removal kinetics of cationic azo-dye from aqueous solution by poly-γ-glutamic acid biosorbent: contributions of adsorption and complexation/precipitation to basic orange 2 removal. Journal of Environmental Chemical Engineering, 7: 103157.

Iqbal M.K., Nadeeem A., Shafiq T. (2015): Biological treatment of textile waste water by activated sludge process. Journal of Chemical Society Pakistan, 29: 397–400.

Kang Y., Yoon H., Lee C., Kim E., Chang Y. (2019): Advanced oxidation and adsorptive bubble separation of dyes using MnO_2-coated Fe_3O_4 nanocomposite. Water Research, 151: 413–422.

Nosheen S., Nawaz H., Rehman K.U. (2000): Physico-chemical characterization of effluents of local textile industries of Faisalabad-Pakistan. International Journal of Agriculture and Biology, 3: 232–233.

Tariq J., Ashraf M., Jaffar M., Afzal M. (1996): Pollution status of the Indus River, Pakistan, through heavy metal and macronutrient contents of fish, sediment and water. Water Resource, 30: 1337–1344.

Ullah M., Nazir R., Khan M., Khan W., Shah M., Afridi S.G., Zada A. (2020): The effective removal of heavy metals from water by activated carbon adsorbents of *Albizia lebbeck* and *Melia azedarach* seed shells. Soil and Water Research, 15: 30–37.

Xu B., Zada A., Wang G., Qu Y. (2019): Boosting the visible-light photoactivities of $BiVO_4$ nanoplates by doping Eu and coupling CeO_x nanoparticles for CO_2 reduction and organic oxidation. Sustainable Energy Fuels, DOI:10.1039/C9SE00409B.

Zada A., Qu Y., Ali S., Sun N., Lu H., Yan R., Zhang X., Jing L. (2018): Improved visible-light activities for degrading pollutants on TiO_2/g-C_3N_4 nanocomposites by decorating SPR Au nanoparticles and 2,4-dichlorophenol decomposition path. Journal of Hazardous Materials, 342: 715–723.

Zhou Y., Lu J., Zhou Y., Liu Y. (2019): Recent advances for dyes removal using novel adsorbents: A review. Environmental Pollution, 252: 352–365.

Received: May 31, 2019
Accepted: November 7, 2019
Published online: January 17, 2020